Available online at www.sciencedirect.com
ScienceDirect
Cement and Concrete Research 37 (2007) 1035–1046
Cement and Concrete Research

De-icing salt scaling resistance of mechanically loaded engineered cementitious composites

Mustafa Şahmaran [a], Victor C. Li [b,*]

[a] Department of Civil Engineering, Gaziantep University, 27310 Gaziantep, Turkey
[b] Department of Civil and Environmental Engineering, The University of Michigan, Ann Arbor, MI, 48109, United States

Received 5 September 2006; accepted 4 April 2007

Abstract

This paper reports the durability performance of non-air-entrained Engineered Cementitious Composites (ECC) with different fly ash content when subjected to mechanical loading and freezing and thawing cycles in the presence of de-icing salt. ECC is a newly developed high performance fiber reinforced cementitious composite with substantial benefit in both high ductility in excess of 3% under uniaxial tensile loading and improved durability due to intrinsically tight crack width. After 50 freezing and thawing cycles in the presence of de-icing salt, the surface condition visual rating and total mass of the scaling residue of ECC, even those with high volume fly ash content, remain within acceptable limits according to the ASTM C 672. This level of durability holds true even for specimens pre-loaded to cracking at high deformation level. Non-air-entrained mortar specimens with and without fly ash were also used as reference specimens. As expected, these mortar prisms under identical testing conditions deteriorated severely. Pre-loaded and virgin (no pre-loading) ECC coupon specimens were also exposed to freezing and thawing cycles in the presence of de-icing salts for 25 and 50 cycles to determine their residual tensile behavior. The reloaded specimens showed negligible loss of ductility, but retained the multiple micro-cracking behavior and tensile strain capacity of more than 3%. It is also discovered that multiple micro-cracks due to mechanical loading will heal sufficiently under freezing and thawing cycles in the presence of salt solutions to restore nearly the original stiffness. These results confirmed that ECC, both virgin and micro-cracked, remain durable despite exposure to freezing and thawing cycles in the presence of de-icing salts.

Keywords: Engineered Cementitious Composites; Cracking; Freezing and thawing; Scaling; Self-healing

1. Introduction

An increasing problem in the United States is the maintenance and rehabilitation of the infrastructure. Deterioration occurs more rapidly in northern regions because of the cold weather during the winter. It is well known that the widespread use of de-icing salts during winter is one of the major causes of the rapid degradation of concrete pavements, bridge decks, parking structures, and similar structures. De-icing salt, employed to lower the freezing point of water, is usually used by spreading it on the surface of concrete roads in winter for driver safety. In these cold weather environments, concrete deterioration is accelerated because it is subjected to de-icing salt under freezing and thawing cycles. When a de-icing salt is applied under freezing and thawing cycles on concrete structure, the destructive phenomena of scaling, cracking, or other erosive effects will occur in the surface layer of concrete structures [1]. The deterioration due to de-icing salt's erosive effect can develop rather rapidly compared with the destructive effect of normal freezing and thawing cycling process in concrete. In addition to reducing the serviceability of the structure, surface scaling is known to favor the ingress of deleterious chemicals into the interior of the concrete [2] which consequently increases the risk of deterioration by other phenomena such as corrosion of reinforcing steel.

The mechanisms related to the scaling of concrete surfaces due to freezing in the presence of de-icing salts are still not fully understood [1,3]. Factors that can influence salt scaling resistance of concrete include: air-void structure, the level of

* Corresponding author. Tel.: +1 734 764 3368; fax: +1 734 764 4292.
E-mail address: vcli@umich.edu (V.C. Li).

0008-8846/$ - see front matter © 2007 Elsevier Ltd. All rights reserved.
doi:10.1016/j.cemconres.2007.04.001

saturation of concrete, compressive strength, water–cementitious materials ratio (W/CM), type and amount of mineral admixtures (fly ash, slag, etc.), type and amount of chemical admixtures, aggregate type and gradation, finishing and curing procedures, and exposure conditions [1]. The most important factor with regard to frost salt scaling resistance is the air-void structure. Several parameters determine the air-void profile of a concrete structure. Air content, spacing factor and specific surface are considered key parameters according to the national standards e.g. ASTM C 457 [4].

Numerous laboratory test data [see, e.g. [5,6]] in accordance with ASTM C 672 have indicated that air-entrained concretes incorporating high volume fly ash often perform unsatisfactorily when exposed to freezing and thawing cycles in the presence of de-icing salts. Regardless of the type of fly ash used the concrete exhibits severe scaling with a visual rating of 5 according to ASTM C 672. On the other hand, there are several reported cases of concrete structures incorporating significant amounts of the fly ash that have performed well when exposed to de-icing salts in the field [7]. It is believed that ASTM C 672 is an overly severe test for determining the de-icing salt scaling resistance of high volume fly ash concrete in actual field application [7]. So far there is no clear explanation for this discrepancy between laboratory observation and field experience. For the production of Engineered Cementitious Composite (ECC), as much as two-thirds of the portland cement is substituted by fly ash. Due to the high volume fly ash content, it is important to test the performance of ECC exposed to freezing and thawing cycles in the presence of de-icing salt.

ECC is a fiber reinforced cement based composite material micro-mechanically tailored by the addition of short fibers so as to achieve high ductility and multiple cracking under tensile and shear loading [8–10]. Unlike ordinary concrete materials, ECC strain-hardens after first cracking, similar to a ductile metal, and demonstrates a strain capacity 300–500 times greater than normal concrete. Even at large imposed deformation, crack widths of ECC remain small, less than 70 μm. The tight crack width of ECC is important to the durability of ECC structures as the tensile ductility is to the structural safety. These properties, together with a relative ease of production including self-consolidation casting and shotcreting, make ECC suitable for various civil engineering applications [11,12].

Concrete in real structures is always cracked. Cracking is usually a result of various physical and chemical interactions between concrete and its environment, and it may develop at different stages throughout the life of the structure. Durability is of increasing concern in the concrete industry, and it is significantly affected by the presence of cracks. Cracks can reduce the strength and stiffness of the concrete structure and accelerate the ingress of aggressive ions, leading to other types of concrete deterioration and resulting in further cracks [13]. Concrete shrinkage, thermal deformations, chemical reactions, poor construction practices and mechanical loads are some of the reasons of cracks in concrete [14]. Unlike conventional concrete and most fiber reinforced concretes, ECC exhibits self-controlled crack widths under increasing load. Even at ultimate load, the crack width remains less than 70 μm, regardless of the amount of steel reinforcements. This study was undertaken to obtain more information on the de-icing salt scaling resistance of ECC particularly in the presence of micro-cracking. Although the limited field performance of ECC generally indicates that it has a good frost and de-icing salt scaling resistance [15], no quantitative data has been published in the scientific and technical literature on this subject. Such information is important in view of the growing use of ECC, especially for road pavement and bridge decks in cold climate regions. In the present research, experimental work was conducted on non-air-entrained ECC beams and coupon specimens pre-cracked to different deformation levels. The micro-cracked specimens were then exposed to freezing and thawing cycles in the presence of de-icing salts. In addition to ECC, the resistance of non-air-entrained mortar mixtures with and without fly ash to cycles of freezing and thawing in the presence of de-icing salts was also measured in a control test series.

In the following, details of experimental studies, including materials, mixture proportions and specimen preparation, are described. Information on the salt scaling test and uniaxial tension test, are then documented. This is followed by a summary and discussions of test results. The paper ends with specific conclusions drawn from this experimental investigation.

Table 1
Mechanical and geometrical properties of PVA fiber

Nominal strength (MPa)	Apparent strength (MPa)	Diameter (μm)	Length (mm)	Young's modulus (GPa)	Elongation (%)
1620	1092	39	8	42.8	6.0

Table 2
Mixture properties of ECC and mortar

	ECC-1 (M45)	ECC-2	Mortar-1	Mortar-2
FA/C	1.2	2.2	–	0.4
W/CM [a]	0.27	0.27	0.35	0.35
Water (W), kg/m^3	331	327	215	215
Cement (C), kg/m^3	570	386	614	430
Fly ash (FA), kg/m^3	684	847	–	185
Sand (S), kg/m^3	455	448	1535	1486
Fiber (PVA), kg/m^3	26	26	–	–
HRWR, kg/m^3	4.9	3.7	–	–
Fresh air content (without PVA fiber) (%)	3.8	4.0	2.9	3.1
Fresh air content (with PVA fiber) (%)	8.7	9.3	–	–
7-day compressive strength, MPa	38.1	21.6	38.4	28.3
28-day compressive strength, MPa	50.2	36.3	49.0	35.7

[a] CM: cementitious materials (cement + fly ash).

2. Experimental studies

2.1. Materials, mixture proportions, and specimen preparation

The materials used in ECC mixtures were ordinary portland cement (C), Class-F fly ash (FA) with a lime content of 10.44%,

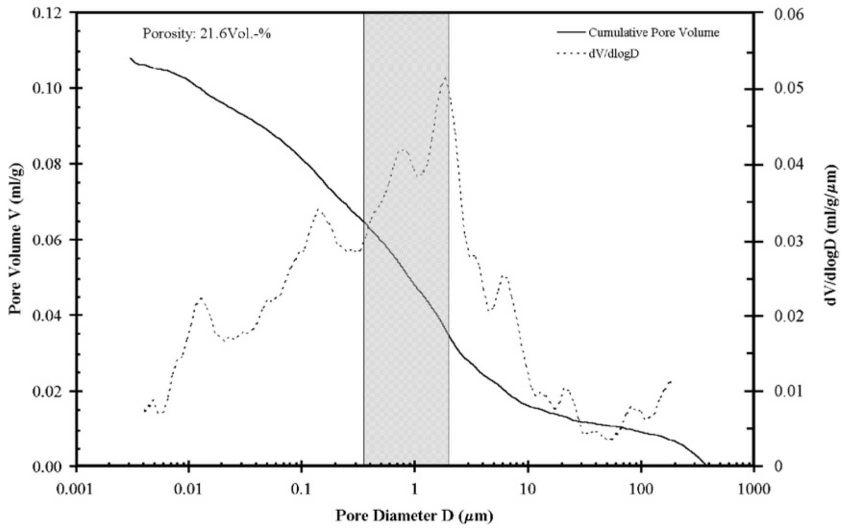

Fig. 1. Pore size distribution of ECC-1 (M45).

silica sand with an average and maximum grain size of 110μm and 200μm respectively, water, poly-vinyl-alcohol (PVA) fibers, and a high range water reducing admixture (HRWR). The PVA fibers are purposely manufactured with a tensile strength, elastic modulus, and maximum elongation matching those needed for strain-hardening performance [16]. Additionally, the surface of the PVA fibers is coated 1.2% by weight with a proprietary hydrophobic oiling agent to tailor the interfacial properties between fiber and matrix for strain-hardening performance. The mechanical and geometrical properties of the PVA fibers used in this study are shown in Table 1.

Two ECC mixtures were used in this investigation, details of which are given in Table 2. ECC mixtures were prepared in a standard mortar mixer at a constant amount of cementitious material and constant water to cementitious material (W/CM) ratio of 0.27. ECC mixtures had a fly ash–cement ratio (FA/C) of 1.2 and 2.2 by mass. HRWR was added to the mixture until the desired fresh ECC characteristics were visually observed; therefore, the HRWR admixture content was not kept constant. In a control test series, two types of mortar mixtures were also studied: portland cement mortar without fly ash (designated Mortar-1); and portland cement mortar with fly ash (designated Mortar-2). The mixture proportions of the mortars are also shown in Table 2. All materials in this study, ECC and mortar, contain no air-entraining admixture.

Mercury intrusion porosimetry was used to characterize the pore size distribution of ECC. A typical pore size distribution curve is shown in Fig. 1 for an ECC-1 (M45) sample. As seen from this Figure, a large number of pores in the target range between 0.35 μm and 2.00 μm have been observed. Furthermore, the large porosity value of 21.6% seen from Fig. 1 indicates that a large number of these small pores exist. From this pore distribution curve, good frost resistance can be expected from all ECC specimens. Additionally, the spacing factor is the most critical factor affecting frost resistance. Using the cumulative distribution curve (Fig. 1), total porosity value

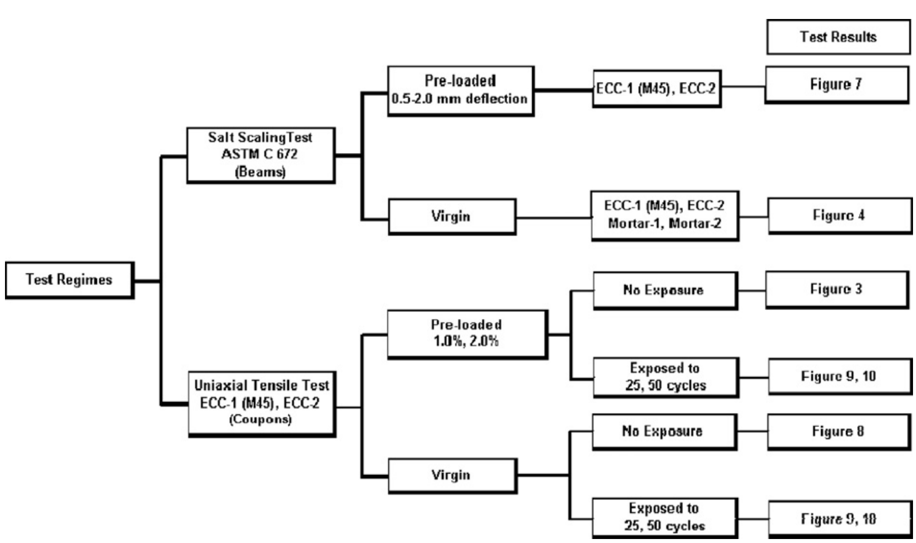

Fig. 2. Flow chart for experimental program.

Table 3
Crack widths and numbers of pre-cracked ECC prisms

Mix ID	Beam deformation (mm)	Average crack widths (ìm)	Crack number
ECC-1 (M45)	0.5	–	–
	1.0	~40	8
	1.5	~50	14
	2.0	~50	26
ECC-2	0.5	–	–
	1.0	~10	13
	1.5	~30	21
	2.0	~30	49

Table 4
Crack numbers and average crack widths of pre-cracked ECC coupons

Mix ID	Pre-loading tensile strain (%)	Average crack widths (μm)	Crack number
ECC-1 (M45)	1.0	~44	12
	2.0	~55	21
ECC-2	1.0	~30	16
	2.0	~38	25

(21.6 vol. %) and assumed spherical pore of 2 μm mean diameter, the average spacing factor was found to be significantly less than 50 μm. The total porosity value of ECC was determined by mercury intrusion porosimetry. The estimated spacing factor is well below the usual recommended value for good frost resistance (200 μm) in concrete [17]. This phenomenon is mostly due to the fact that the air content of the mixtures increases with the addition of PVA fibers and with the lack of coarse aggregate. As explained by Powers [18], the fine aggregate particles tend to prevent some of the air bubbles from rising to the surface during the placing operations. The air contents measured during fresh state of ECC mixtures show that this phenomenon is amplified after the addition of PVA fiber to the mixtures (Table 2). For the above reasons, no air-entrainment was applied to the ECC specimens in the freeze–thaw cycle tests. For comparison purpose, and for ensuring that the test methods were properly applied, the control test used mortar were also not air-entrained.

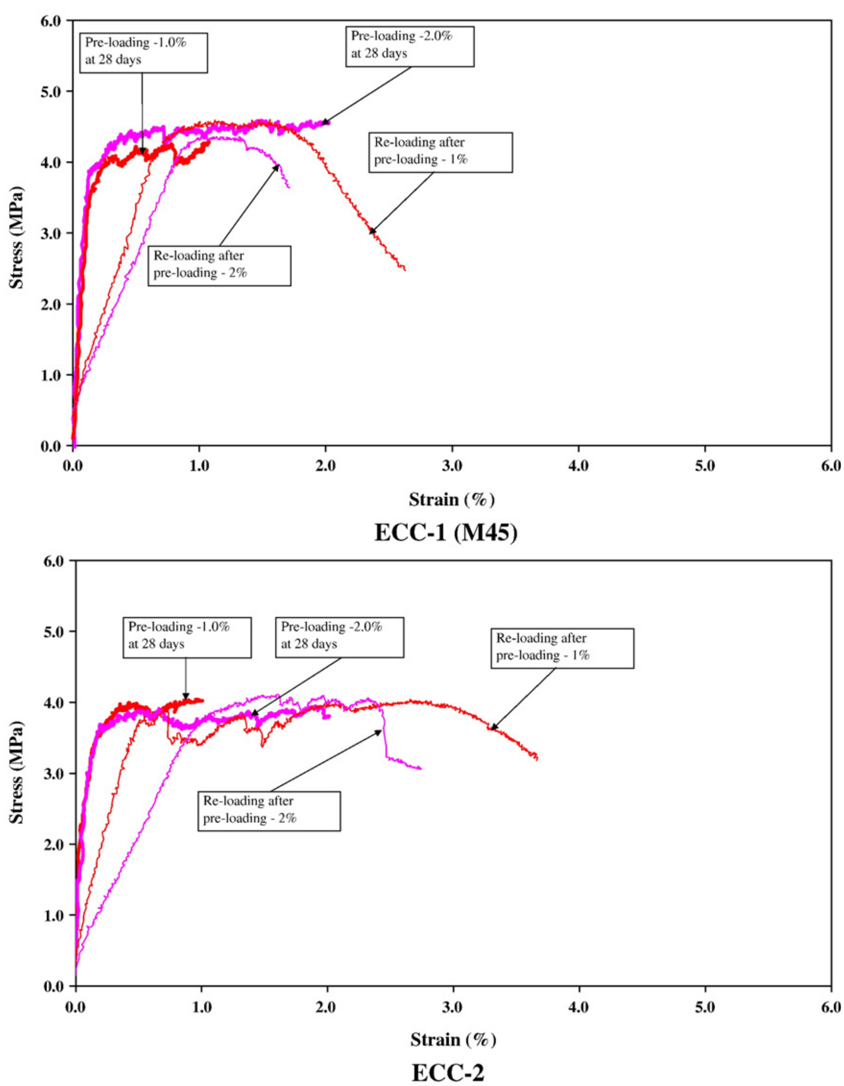

Fig. 3. A typical tensile stress–strain curves for pre-loading and reloading at 28 days.

Table 5
De-icing salt scaling test results of ECC and mortar after 50 cycles

Mix ID	Beam deformation (mm)	Average crack widths (μm)	Crack number	Scaled-off particles (kg/m^2)	Visual ratings (ASTM C 672)
Mortar-1	–	–	–	2.16	5
Mortar-2	–	–	–	4.15	5
ECC-1	–	–	–	0.40	1
(M45)	0.5	–	–	0.52	2
	1.0	~40	8	0.40	1
	1.5	~50	14	0.57	2
	2.0	~50	26	0.71	2
ECC-2	–	–	–	0.35	1
	0.5	–	–	0.42	1
	1.0	~10	13	0.51	2
	1.5	~30	21	0.86	2
	2.0	~30	49	1.13	3

The compressive strength test results of ECC and mortar mixtures are also listed in Table 2. The compressive strength was computed as an average of three standard ∅75×150-mm cylinder specimens. As seen from Table 2 and as expected, the compressive strength of ECC and mortar decreased with increasing fly ash content.

From each mixture, 355.6×50.8×76.2 mm prism specimens were prepared for the de-icing salt scaling test. 152.4×76.2×12.7 mm coupon specimens were also prepared for the direct uniaxial tensile test for the ECC mixtures. All specimens were demolded at the age of 24 h, and moisture cured in plastic bag at 95±5% RH, 23±2 °C for 14 days. The specimens were then air cured in laboratory medium at 50±5% RH, 23±2 °C until the age of 28 days for testing in accordance with ASTM C 672.

The complete testing program is summarized in Fig. 2, and detailed below.

2.2. De-icing salt scaling test

The ASTM C 672 "Standard Test Method for Scaling Resistance of Concrete Surfaces Exposed to De-icing Chemicals" test method is the most common standardized laboratory test designed to assess the scaling resistance of concrete surfaces exposed to frost in the presence of de-icing chemicals [19]. In this experimental study, ASTM C 672 was utilized to assess the performance of ECC prism surfaces when subjected to the combined attack of frost and de-icing salts. This test was used to determine the resistance to scaling when a horizontal surface of a specimen is exposed to de-icing salts and repeated freezing and thawing cycles.

At the age of 28 days, the ECC prisms were pre-cracked up to 2.0 mm deformation level using four-point bending test to obtain different crack widths. The 2.0 mm deformation is nearly equivalent to 1.5% strain on the tensile face of the beam. The salt scaling test was carried out with the pre-loaded ECC specimens in the unloaded state. Two ECC beams were tested for each deformation level. A small amount of crack closure occurred on unloading. To account for this, all crack width measurements were conducted in the unloaded stage. The widths of the crack were measured on the tension face of the ECC prisms by an optical microscope. Cracks with widths below 50 μm were distributed on the surface of the ECC specimens as a result of the bending pre-load. Table 3 shows the pre-cracked beam deformation (BD) value, their corresponding average crack widths (CW), and number of cracks for ECC prism specimens. On the other hand, after the bending load application, one single macro crack was present in the mortar specimens and the crack propagated rapidly through the specimen due to the brittle nature of mortar. As a result, it was not possible to hold the de-icing solution on the cracked surface of the pre-cracked mortar specimens. For this reason, only virgin mortar specimens were tested for determining the de-icing salt scaling resistance of mortar mixtures. Two virgin prisms from each mixture were tested for control purpose.

To determine scaling resistance, plexiglass was placed around the side surfaces of the prism to build a dike for holding chloride solution on the exposed surface of prisms. The de-icing agent (4% sodium chloride solution) was contained on the cracked surface of prisms (355.6×50.8=180.65 cm^2 of exposed surface area) during continuous cycles of freezing and thawing. During freezing, prism specimens were stored at temperature of −18±3 °C for 18 h. At the end of each freezing

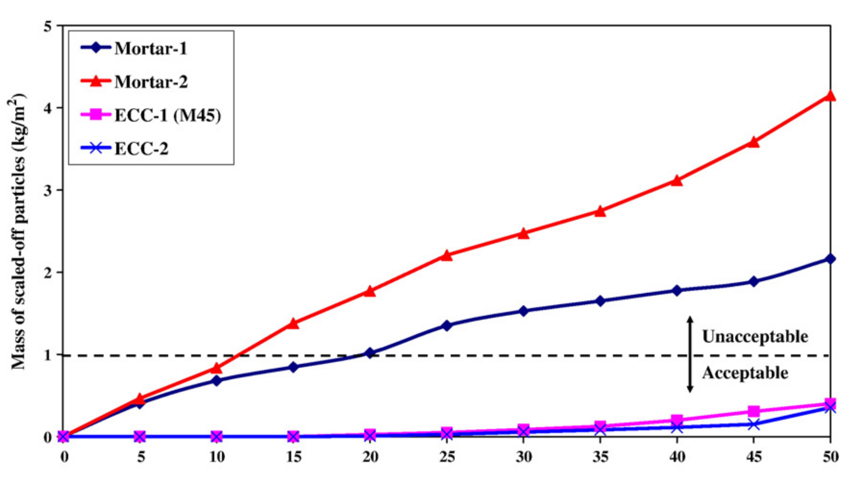

Fig. 4. Mass of scaled-off particles versus number of cycles for virgin mortar and virgin ECC prisms.

Fig. 5. De-icing salt surface scaling after 50 freezing and thawing cycles of virgin ECC and mortar specimens.

period they were placed in the laboratory medium (23±3 °C) to thaw for 6 h. In between each freezing and thawing cycle, sodium chloride solution was added to maintain the proper depth (6 mm) of solution. In addition to visual rating of surface conditions in accordance with ASTM C 672 (0, no scaling to 5, severe scaling), the surface scaling residues were collected and weighed at the end of every five cycles up to 50 cycles to evaluate deterioration. The weight of scaled-off residue can be considered the best way to evaluate surface deterioration. It is well known that visual rating is highly subjective and depends on the operator [1]. It cannot, therefore, be used to assess precisely the deterioration due to de-icing salt scaling.

2.3. Uniaxial tensile test

After 28 days of curing, the coupon specimens were pre-cracked to 1.0 and 2.0% direct tensile strain to achieve various amounts of micro-cracks before exposed to de-icing salts under freezing and thawing. Before testing, aluminum plates were glued to both ends of the coupon specimen to facilitate gripping. Tests were conducted on an MTS machine with 25 kN capacity under displacement control at rate of 0.005 mm/s. A typical stress–strain curves obtained when the specimens were mechanically pre-cracked at 28 days before exposure is shown in Fig. 3. When the tensile strain reached the required pre-determined strain value, the tensile load was released. A small amount of crack closure occurred on unloading. To account for this, all crack width measurements were conducted in the unloaded stage. The widths of the crack were measured on the surface of the specimens by an optical microscope. Table 4 shows the pre-loading tensile strain value, their corresponding average crack widths, and number of cracks within the pre-cracked coupon specimens. The gage length used in these measurements was 50 mm. As seen from Table 4, even at large uniaxial tensile strain level (2.0%), crack widths of ECC remain nearly constant, while the number of cracks on tensile surface of the ECC specimens increased. As expected, a higher tensile strain coincides with more cracks.

Fig. 3 shows also the tensile properties of ECC specimens that had been pre-cracked to 1% or 2% strain levels, then unloaded, and immediately reloaded. Thus these specimens had no time to undergo any crack healing which is found in specimens exposed to immersion and freeze–thaw cycles as explained later. As expected, there is a remarkable difference in initial stiffness between virgin specimen and pre-cracked specimen under direct tension. This is due to re-opening of cracks within pre-cracked specimens during reloading [20]. The opening of these cracks offers very little resistance to load, as the crack simply opens to its previous crack width before fiber bridging is re-engaged. Once fiber bridging is re-engaged, however, the load capacity resumes, and further tensile straining of the intact material can take place.

Immediately after pre-cracking, the pre-cracked ECC coupon specimens were subjected to immersion and freezing exposure cycles. Each cycle is composed of immersion of

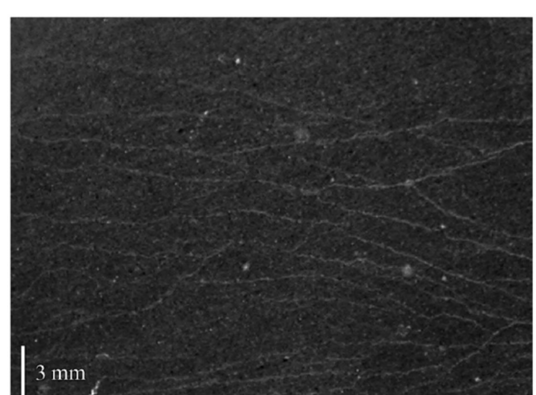

Fig. 6. Typical crack pattern on negative moment surface of ECC beams after bending load application.

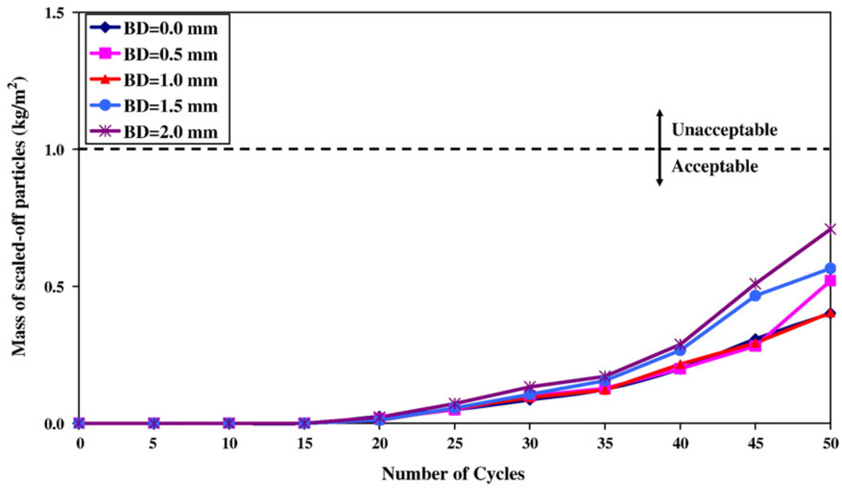

(a) ECC-1 (M45)

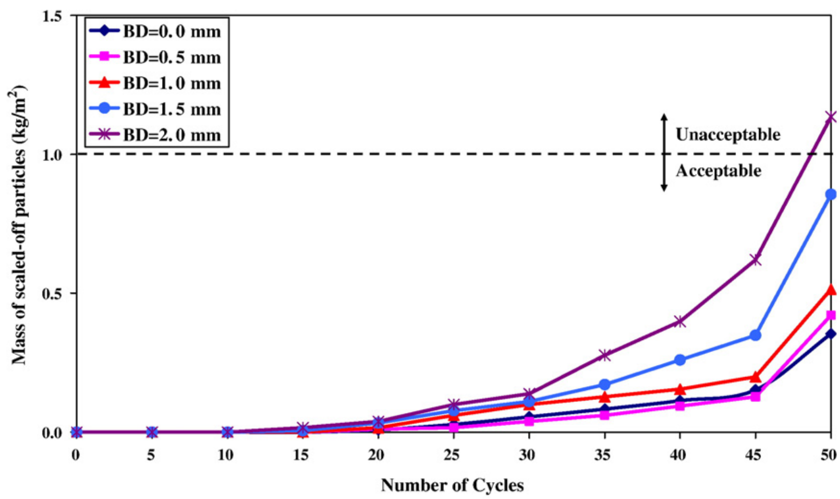

(b) ECC-2

Fig. 7. Mass of scaled-off particles versus number of cycles for ECC mixtures.

specimens in 4% NaCl solution at room temperature (23 ± 3 °C) for 6 h and then saturated coupon specimens were placed at temperature of −18 ± 3 °C for 18 h. Each complete cycle therefore represents one day of exposure. The de-icing salt solution was replaced with a fresh solution at the end of every seven cycles. Reloading under direct tension of specimens having exposed to 25 and 50 exposure cycles was conducted and their stress–strain curves were recorded. For control purpose, virgin specimens were also tested after 25 and 50 days additional curing in laboratory condition (50 ± 5% RH, 23 ± 2 °C). The average tensile strain capacity, ultimate tensile strength and residual crack width of pre-loaded and virgin ECC for each exposure period were calculated from five specimens.

3. Results and discussions

3.1. Resistance to frost with de-icing salts

The visual rating in accordance with ASTM C 672 and weight of scaled-off residues after 50 freezing and thawing cycles are shown in Table 5. Every five cycles, surfaces were rated and all the residues that scaled-off from the surfaces were collected. The scaled-off residue was placed in an oven at 100 °C and weighed after 24 h drying. An ECC or mortar is considered to be durable if the total mass of scaling residue is below 1 kg/m^2 after 50 freezing and thawing cycles [1,21].

As seen from Table 5, the virgin ECC prisms showed good performance when exposed to freezing and thawing cycles in the presence of de-icing salts and, even after 50 cycles, a maximum of only 0.40 kg/m^2 of scaled-off particles was measured for these specimens. This can also be observed in Fig. 4 where the relation between the mass of scaled-off particles and number of cycles is shown for ECC specimens that were subjected to 50 cycles. Little or no scaling could be measured throughout the first fifteen cycles of scaling (Fig. 4). From this time forward, very slight scaling was observed on the ECC prism surface. The ECC sample survived the entire series of fifty scaling cycles. On the other hand, non-air-entrained mortar mixtures with and without fly ash exhibited severe surface scaling after 50 cycles of freezing and thawing. In particular, mortar specimens made from the fly ash mixture

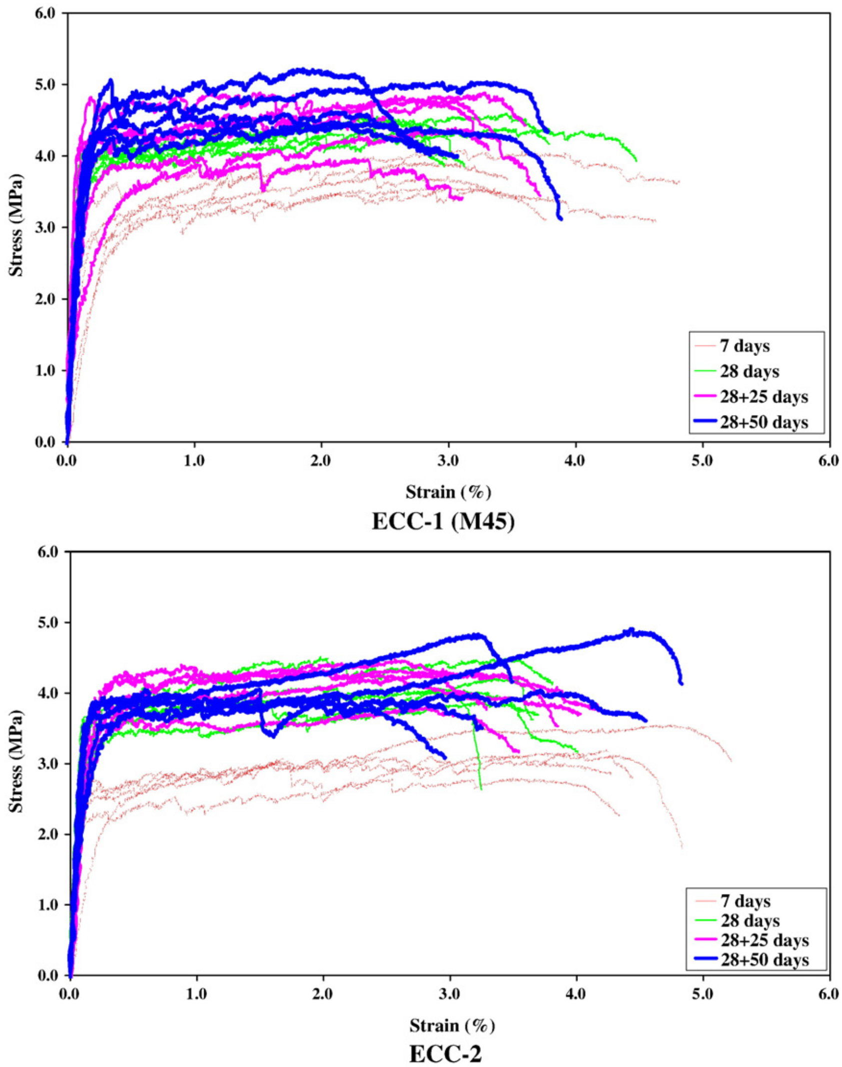

Fig. 8. Tensile behavior of ECC mixtures cured in air after 14 days moist curing.

showed a very high amount of scaled-off residue with a value of 4.15 kg/m^2 at the end of 50 cycles. This finding is consistent with previous knowledge. Fig. 5 shows the typical surface condition of virgin ECC and mortar specimens after 50 cycles of freezing and thawing in the presence of de-icing salt. As seen from these photos, a large portion of the virgin ECC surface remained intact at the end of 50 cycles while those of the mortar specimen surface showed severe scaling damage. Therefore, ECC with innately high air content and low spacing factor tend to have a high scaling resistance despite no deliberate air-entrainment as is required for normal concrete and mortar.

Cracking in ECC is fundamentally different from that which occurs in concrete or reinforced concrete. ECC develops multiple micro-cracking in a strain-hardening response as a result of the bending pre-load (Fig. 6). Due to multiple micro-cracking, it is important to test the pre-cracked ECC under freezing and thawing cycles in the presence of de-icing salt. The average total mass of scaled-off material versus number of freezing–thawing cycles for each ECC mixture at different beam deformation (BD) level is shown in Fig. 7. The total mass of scaling residue of virgin (BD = 0 mm) ECC specimens exposed to freezing and thawing cycles in the presence of de-icing salt is also included in this figure. It can be observed that the total mass of scaling residue after 50 cycles tends to increase with an increase in the imposed beam deformation level. The increase, however, is fairly insignificant for ECC specimens at different deformation levels. On all specimens, a large proportion of the surface remained intact during the tests even though a rating of three was given to the specimen shown in Table 5. This increase is somewhat more marked for ECC incorporating FA/C ratio of 2.2 (ECC-2). After 50 cycles, the highest loss of mass is 1.13 kg/m^2 for ECC-2 pre-loaded to 2 mm flexural deformation. This is a little above the acceptable limit of 1 kg/m^2.

In general, for concretes of the same W/CM ratio, made with the same amount of cementitious material, having the same air content, the incorporation of fly ash increases the mass of scaling residue. It is also known that a proper air-void system is needed in normal concrete to avoid internal cracking due to freezing and thawing cycles and scaling due to freezing in the

Table 6
Summary of tensile stress–strain tests for ECC-1 (M45) specimens

Specimen type		Tensile strain (%)	Tensile strength (MPa)	Residual crack width (im)
Specimens cured in laboratory air after 14 days moist curing	7 days	3.48 [0.41]	3.73 [0.23]	66.60 [25.00]
	28 days	3.16 [0.68]	4.45 [0.11]	48.30 [27.90]
	28 days+ 25 days	3.075 [0.29]	4.456 [0.43]	45.60 [12.00]
	28 days+ 50 days	2.93 [0.56]	4.73 [0.33]	38.40 [16.00]
Specimens subjected to freezing and thawing in the presence of de-icing salt	Uncracked, 25 cycles	2.91 [0.23]	4.17 [0.19]	63.90 [8.97]
	Uncracked, 50 cycles	3.23 [0.69]	4.29 [0.21]	85.40 [19.91]
	pre-cracked—1.0%, 25 cycles	3.14 [0.82]	4.02 [0.32]	82.30 [25.66]
	Pre-cracked—1.0%, 50 cycles	3.16 [0.64]	4.086 [0.33]	88.70 [18.60]
	Pre-cracked—2.0%, 25 cycles	3.25 [0.35]	4.16 [0.17]	61.60 [21.04]
	Pre-cracked—2.0%, 50 cycles	3.24 [0.53]	4.26 [0.36]	78.90 [7.37]

Numbers in parentheses are standard deviations.

presence of de-icing salts. In the case of ECC, the presence of the natural air-void system with low average spacing factor as described earlier and micro PVA fiber, appears to be responsible for enhancing the frost and de-icing salt scaling resistance, as revealed in this series of tests. The influence of micro-fiber addition on the resistance of concrete to the effect of de-icing salts scaling has also been examined by other researchers [22,23], and is consistent with the current findings. It is plausible that micro-fibers aid in arresting the micro-cracks in the matrix induced by internal pressures built up by frost action.

3.2. Uniaxial tensile test

Fig. 8 shows the tensile behavior of ECC mixtures cured in air at different ages, after an initial 14 days moist curing. These ECC composites exhibited a strain capacity of more than 3% at 28 days. The strain capacity measured after 28 days is slightly lower than the 7-day strain capacity (Fig. 8 and Tables 6 and 7) for both types of ECC mixtures; however the observed 3.0% strain capacity remains acceptable for an ECC. The overall effect of this slight drop in long-term strain capacity is minimal. Based on the similarity of test results up to 28 days+50 days, the tensile strain capacity seems to stabilize at 3.0% after 28 days.

Tensile stress–strain curves obtained for coupon specimens pre-cracked at 28 days and subsequently exposed to de-icing salts under freezing and thawing cycles are shown in Figs. 9 and 10. Two sets of data are generated from specimens exposed to 25 and 50 cycles, and two pre-loading levels (1% and 2%) were employed. As seen in these figures, the first-cracking strength of ECC specimens after cyclic exposure falls below the first-cracking strength of the virgin specimens cured in air. Another distinct observation concerns the shape of the virgin and pre-cracked specimens. In the case of virgin specimens, the initial shape of the curves is almost linear up to about 90% of ultimate tensile load. The initial linear portion of the stress–strain curves of the pre-cracked specimens, however, extends only up to about 50% of the ultimate load. Nevertheless, no significant reduction on tensile strain capacity of the ECC specimens exposed to de-icing salts under freezing and thawing can be detected.

By comparing the initial material stiffness of reloaded ECC specimens exposed to freezing and thawing cycles in the presence of de-icing salts in Figs. 9 and 10 with that shown for the reloaded specimens before exposure in Fig. 3, it can be observed that a significant recovery of mechanical stiffness has been achieved. This suggests that between the time of inducing pre-cracking and the time of testing, after freezing and thawing cycles in the presence of salt solution, healing of the micro-cracks has occurred in the ECC specimens. This can be attributed primarily to the high cementitious material content and relatively low water to binder ratio within the ECC mixture. As a result of the formation of micro-cracks due to mechanical loading, unhydrated cementitious particles are easily exposed to the sodium chloride solution during the immersion period, which leads to development of further hydration processes. Finally micro-cracks under conditions of a damp environment were closed by newly formed products. These observations are in good agreement with those discussed in the literature [24,25]. These investigations indicated that the formation of re-hydration products in micro-cracks is possible. In ECC, the re-healing process is especially aided by the innately tight crack width.

Table 7
Summary of tensile stress–strain tests for ECC-2 specimens

Specimen type		Tensile strain (%)	Tensile strength (MPa)	Residual crack width (μm)
Specimens cured in laboratory air after 14 days moist curing	7 days	4.21 [0.45]	3.15 [0.27]	35.7 [11.30]
	28 days	3.40 [0.22]	4.07 [0.30]	27.10 [17.04]
	28+25 days	3.37 [0.40]	4.16 [0.28]	26.40 [11.07]
	28+50 days	3.43 [0.84]	4.32 [0.47]	15.00 [5.00]
Specimens subjected to freezing and thawing in the presence of de-icing salt	Uncracked, 25 cycles	3.77 [0.52]	3.69 [0.29]	70.00 [3.00]
	Uncracked, 50 cycles	3.14 [0.56]	3.93 [0.28]	59.50 [8.10]
	Pre-cracked—1.0%, 25 cycles	3.95 [0.78]	3.71 [0.41]	69.28 [16.93]
	Pre-cracked—1.0%, 50 cycles	3.36 [0.57]	3.83 [0.19]	61.80 [16.20]
	Pre-cracked—2.0%, 25 cycles	3.37 [0.71]	3.49 [0.17]	59.17 [11.14]
	Pre-cracked—2.0%, 50 cycles	3.58 [0.29]	3.78 [0.23]	60.26 [15.80]

Numbers in parentheses are standard deviations.

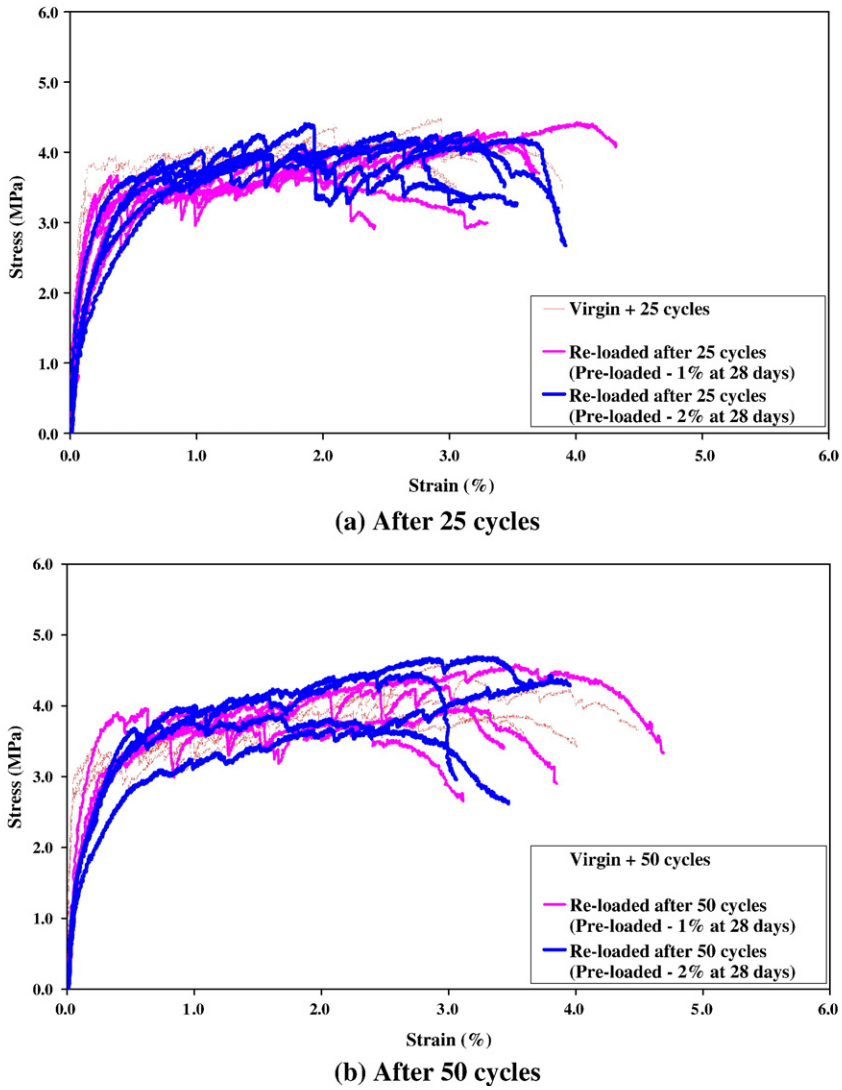

Fig. 9. Effect of freezing and thawing cycles in the presence of de-icing salts on tensile behavior of ECC-1 (M45).

Compared to control specimens cured in laboratory air, the test results (Tables 6 and 7) indicate that the ECC specimens (virgin and pre-cracked) exposed to de-icing salts under freezing and thawing cycles showed reductions of nearly 6% in ultimate tensile strength for all exposure ages; this may be attributed to the effects of damage on the fiber/matrix interface due to freezing and thawing cycles. Note that air cured specimens labeled 28 days + 50 days would have the same age as exposed specimens labeled 28 days + 50 cycles, since each complete cycle of exposure takes 24 h.

Tables 6 and 7 summarize the average of tensile strain capacity of ECC specimens exposed to de-icing salts under freezing and thawing cycles. The tensile strain capacity reported for these specimens does not include the residual strain from the pre-cracking load. By neglecting this residual strain, the large variability in material relaxation during unloading is avoided, and a conservative estimation for ultimate strain capacity of the material is presented. The tensile strain capacity of virgin and pre-cracked ECC specimens exposed to de-icing salts under freezing and thawing cycles range from 2.91% to 3.95%. The exposed ECC specimens retain at least the strain capacity of ECC specimens unexposed to freezing and thawing cycles in the presence of de-icing salt.

Tables 6 and 7 also show the residual crack width of ECC mixtures at different ages. The term residual crack width indicates that crack width was measured from the unloaded specimen after the uniaxial tensile test by using optical microscope. Each average crack width in Tables 6 and 7 was an average of those measured in 5 coupon specimens. The residual crack width of virgin and pre-cracked specimens exposed to de-icing salts under freezing and thawing cycles is wider than that of virgin air cured specimens, but remains less than 100 μm. In terms of permeability, crack width less than 100 μm generally behave like sound concrete [26]. Based on experimental results, Evardsen [27] and Reinhardt and Jooss [28] proposed that cracks with width below 100 μm can be easily closed by a self-healing process. However, more experimental studies on a micro-mechanical scale are necessary

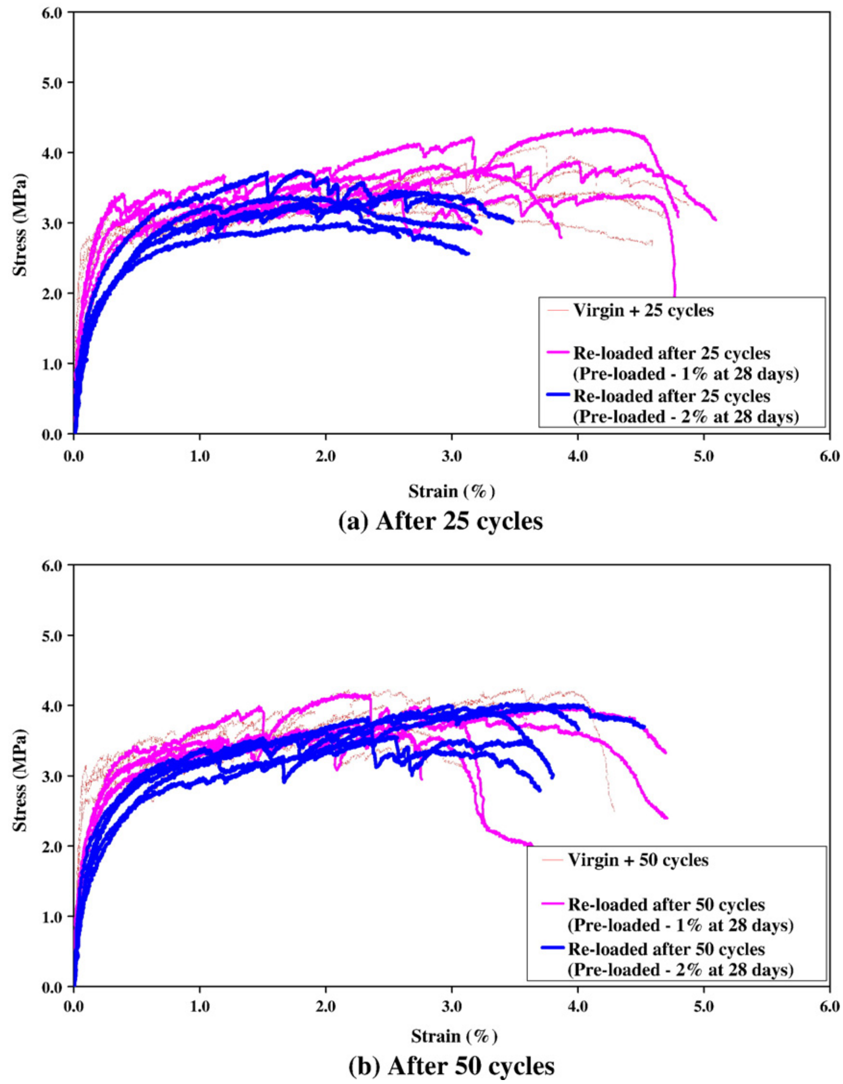

Fig. 10. Effect of freezing and thawing cycles in the presence of de-icing salts on tensile behavior of ECC-2.

to clearly understand the mechanisms behind the reduction in the ultimate tensile strength and increased crack width, and are beyond the scope of this paper.

4. Conclusion

The ASTM C 672 scaling test results described in this paper show that non-air-entrained virgin ECC made with high volume fly ash performed satisfactorily. For the virgin ECC specimens, scaled-off particles less than 0.40 kg/m^2 were determined. For the pre-loaded (pre-cracked) ECC specimens, the magnitude of beam deformation level was found to have little detrimental effect since even for a 2 mm beam deformation level (equivalent to prestraining to 1.5% on the exposed tensile face), very good salt scaling resistance was obtained. Only the mass of scaling residue of ECC mixtures with FA/C ratio of 2.2 and beam deformation value of 2.0 mm exceeded the 1 kg/m^3 acceptable limit in this severe scaling test.

Uniaxial tensile specimens pre-cracked up to 2.0% strain showed almost complete recovery of stiffness when re-tested in direct tensile stress even after fifty freezing and thawing cycles in the presence of de-icing salt. The tensile strain capacity of these exposed virgin and pre-cracked ECC specimens is at least as high as that for virgin specimens cured in air although they experience about 6% loss in ultimate tensile strength and an increase in residual crack width to less than 100 μm on reloading. Healing of micro-cracks induced by the pre-load is evident from the recovery of elastic stiffness of the exposed pre-cracked specimens on reloading.

Apart from the slight reduction in ultimate tensile strength and higher residual crack width, the results presented in this study largely confirm the durability performance of ECC material under freezing and thawing cycles in the presence of de-icing salts, even in cases where the material experiences mechanical loading that deforms it into the strain-hardening stage prior to exposure. In addition, the scaling resistance of ECCs was not significantly influenced by the fly ash content, at least within the range studied. This durability of ECC under freezing and thawing in the presence of de-icing salt was achieved without deliberate air entrainment.

Acknowledgments

The first author would like to acknowledge the financial support of TUBITAK (The Scientific and Technical Research Council of Turkey). This research was partially funded through an NSF MUSES Biocomplexity Program Grant (CMS-0223971 and CMS-0329416). MUSES (Materials Use: Science, Engineering, and Society) supports projects that study the reduction of adverse human impact on the total interactive system of resource use, the design and synthesis of new materials with environmentally benign impacts on biocomplex systems, as well as the maximization of efficient use of materials throughout their life cycles.

References

[1] M. Pigeon, R. Pleau, Durability of Concrete in Cold Climates, Chapman & Hall, London, 1995.
[2] J.J. Valenza, G.W. Scherer, Mechanism for salt scaling, J. Am. Ceram. Soc. 89 (4) (2006) 1161–1179.
[3] J. Marchand, E.J. Sellevold, M. Pigeon, The deicer salt scaling deterioration of concrete — an overview, Durability of Concrete, SP-145, American Concrete Institute, 1994, pp. 1–46.
[4] ASTM C 457-98, Standard Test Method for Microscopical Determination of Parameters of the Air-Void System in Hardened Concrete, American Society for Testing and Materials, Philadelphia, 2001.
[5] A. Bilodeau, V. Sivasundaram, K.E. Painter, V.M. Malhotra, Durability of concrete incorporating high volumes of fly ash from sources in the U.S. ACI Mater. J. 91 (1) (1994) 3–12.
[6] N. Bouzoubaa, B. Fournier, V.M. Malhotra, D.M. Golden, Mechanical properties and durability of concrete made with high-volume fly ash blended cement produced in cement plant, ACI Mater. J. 99 (6) (2002) 560–567.
[7] V.M. Malhotra, P.K. Mehta, High-performance, high-volume fly ash concrete: materials, mixture proportioning, properties, construction practice, and case histories, Supplementary Cementing Materials for Sustainable Development, Ottawa, Canada, 2005.
[8] V.C. Li, ECC-Tailored composites through micromechanical modeling, in: Banthia, et al., (Eds.), Fiber Reinforced Concrete: Present and the Future, CSCE, Montreal, 1998, pp. 64–97.
[9] V.C. Li, On Engineered Cementitious Composites (ECC) — a review of the material and its applications, J. Adv. Concr. Technol. 1 (3) (2003) 215–230.
[10] V.C. Li, S. Wang, C. Wu, Tensile strain-hardening behavior of PVA-ECC, ACI Mater. J. 98 (6) (2001) 483–492.
[11] H.J. Kong, S. Bike, V.C. Li, Development of a self-compacting ECC employing electrosteric dispersion/stabilization, Cem. Concr. Compos. 25 (3) (2003) 301–309.
[12] Y.Y. Kim, H.J. Kong, V.C. Li, Design of Engineered Cementitious Composites (ECC) suitable for wet-mix shotcreting, ACI Mater. J. 100 (6) (2003) 511–518.
[13] P.K. Mehta, B.C. Gerwick, Cracking–corrosion interaction in concrete exposed to marine environment, Concr. Int. 4 (10) (1982) 45–51.
[14] ACI Committee 224R-01, Control of cracking in concrete structures, ACI Manual of Concrete Practice, Part 3, American Concrete Institute, Farmington Hills, Michigan, 2001.
[15] M.D. Lepech, V.C. Li, Long term durability of engineered cementitious composites, Restor. Build. Monum. 12 (2) (2006) 119–132.
[16] V.C. Li, C. Wu, S. Wang, A. Ogawa, T. Saito, Interface tailoring for strain-hardening PVA-ECC, ACI Mater. J. 99 (5) (2002) 463–472.
[17] T.C. Powers, The air requirement of frost-resistant concrete, Proceedings, Highway Research Board, Washington, D.C., vol. 29, 1949, pp. 184–202.
[18] T.C. Powers, J. PCA Res. Dev. Lab. 6 (1964) 19.
[19] ASTM C 672-98, Standard Test Method Scaling Resistance of Concrete Surfaces Exposed to De-icing Chemicals, American Society for Testing and Materials, Philadelphia, 2001.
[20] Y. Yang, M.D. Lepech, V.C. Li, Self-healing of ECC under cyclic wetting and drying, Proceedings of Int'l. Workshop on Durability of Reinforced Concrete under Combined Mechanical and Climatic Loads, Qingdao, China, 2005, pp. 231–242.
[21] SS 127244, Concrete Testing Hardened Concrete Frost Resistance, Swedish Standards Commission, 1988.
[22] M. Pigeon, M. Azzabi, R. Pleau, Can microfibers prevent frost damage? Cem. Concr. Res. 26 (8) (1996) 1163–1170.
[23] J. Deja, Freezing and de-icing salt resistance of blast furnace slag concretes, Cem. Concr. Compos. 25 (3) (2003) 357–361.
[24] S. Jacobsen, J. Marchand, H. Hornain, SEM observations of the microstructure of frost deteriorated and self-healed concretes, Cem. Concr. Res. 25 (8) (1995) 1781–1790.
[25] A. Mor, P.J.M. Monteiro, W.T. Hester, Observations of healing of cracks in high-strength lightweight concrete, Cem. Concr. Aggreg. 11 (2) (1989) 121–125.
[26] K. Wang, D. Jansen, S. Shah, A. Karr, Permeability study of cracked concrete, Cem. Concr. Res. 27 (3) (1997) 381–393.
[27] C. Evardsen, Water permeability and autogenous healing of cracks in concrete, ACI Mater. J. 96 (4) (1999) 448–454.
[28] H.W. Reinhardt, M. Jooss, Permeability and self-healing of cracked concrete as a function of temperature and crack width, Cem. Concr. Res. 33 (7) (2003) 981–985.